Exotic silicon phases synthesized through ultrashort laser-induced microexplosion: Characterization with Raman microspectroscopy

L. A. Smillie,[1,2,*] M. Niihori [ORCID],[2] L. Rapp,[1] B. Haberl [ORCID],[3] J. S. Williams,[2] J. E. Bradby,[2] C. J. Pickard,[4,5] and A. V. Rode[1,†]

[1]*Laser Physics Centre, Research School of Physics, The Australian National University, Canberra ACT 2601, Australia*
[2]*Department of Electronic Materials Engineering, Research School of Physics, The Australian National University, Canberra ACT 2601, Australia*
[3]*Neutron Scattering Division, Neutron Sciences Directorate, Oak Ridge National Laboratory, Oak Ridge, Tennessee 37831, USA*
[4]*Department of Materials Science and Metallurgy, University of Cambridge, Cambridge CB3 0FS, United Kingdom*
[5]*Advanced Institute for Materials Research, Tohoku University, Aoba, Sendai, 980-8577, Japan*

Exotic metastable phases of silicon formed under high pressure are expected to have attractive semiconducting properties including narrow band gaps that open up novel technological applications. Confined microexplosions induced by powerful ultrashort laser pulses have been demonstrated as an advanced tool for the creation of new high-pressure phases that cannot be synthesized by other means. Tightly focused laser pulses are used to generate localized modifications inside the material structure, providing the possibility for precise controlled band-gap engineering. In this study, noninvasive Raman spectroscopy was used for analysis of laser-modified zones in silicon and to determine the metastable high-pressure phases contained. Low laser energies induced the formation of amorphous-only silicon, while higher energies led to crystalline silicon polymorphs within the modifications, albeit under considerable residual stress up to 4.5 GPa. The presence of the structurally similar r8-Si, bc8-Si, and bt8-Si phases is revealed, as well as other yet to be identified phases, and the stacking-related 9*R* Si polytype is evidenced, presumably stress-induced by the highly compressed laser-modified zone. The *ab initio* random structure searching approach is used to calculate the Raman signatures and to help identify different Si polymorphs. These findings by Raman spectroscopy from ultrashort laser-induced microexplosion sites may yield insights into the local structure and properties of new silicon metastable phases and the prospect of utilizing exotic phases for extending current applications.

I. INTRODUCTION

The discovery of metastable states of matter formed by powerful ultrashort laser pulses demonstrates a new pathway for creating exotic material phases with novel optoelectronic properties [1–6]. Ultrashort laser pulses (in the subpicosecond time domain) focused tightly inside a transparent material can deliver energy at a density of several MJ/cm^3 in a submicron confined volume. Such a level of energy density results in conversion of the laser-heated material to a high-pressure/temperature solid-density plasma, or warm dense matter, where the initial crystalline state is completely destroyed with no memory of the original structural arrangements [4–6]. Relaxation to ambient conditions occurs through intermediate transient states of matter resulting in novel solid metastable phases recovered from high pressure. These phases form with greatly reduced thermodynamic and kinetic constraints compared with those that apply to near-equilibrium diamond anvil cell (DAC) and nanoindentation experiments. The material is subjected to transient pressures in the order of TPa, which is higher than the strength of any material, as well as temperatures in excess of 100 000 K and ultrahigh cooling rates of $\sim 10^{14}$ K/s. At this level of energy concentration, new material phases with a modified energy band gap can be formed, providing a possibility for precise controlled band-gap engineering with tunable band-gap energy [6].

Pressure-induced phase transformations of silicon (Si) have been studied extensively under static pressure conditions, both theoretically and experimentally, because of the potential of these new materials in electronic and photovoltaic devices [7–10]. The microexplosion approach offers the advantage of preservation of the chemical purity of Si and precise control over the size and position of the laser-modified sites. This is unlike the approaches of increasing absorption by surface texturing [11] and by a shift of the band gap via hyperdoping in the presence of gaseous SF_6 [12], or by ion implantation of chalcogens followed by pulsed laser melting [13].

Recently, we evidenced the creation of several novel metastable Si phases by ultrashort laser-induced confined microexplosions, and we demonstrated that these phases are preserved inside the surrounding pristine structure for subsequent studies and utilization [3,14]. Transmission electron microscopy (TEM) revealed tetragonal bt8-Si [with an $I4_1/a$ space group that is structurally an intermediate state between β-Sn-Si ($I4_1/amd$ space group) and bc8-Si (*Ia*-3 space group) [15] and with similarities to both bc8-Si and r8-Si (*R*-3 space

*lachlan.smillie@anu.edu.au
†andrei.rode@anu.edu.au

group) [16] and st12-Si ($P4_32_12$ space group)], which had been previously predicted in Si due to its existence within the very similar Ge system [17,18]. Furthermore, additional Si structures were observed but not characterized, noting that we also predicted four phases with quasidirect band gaps—two monoclinic m32 ($P2_1c$ space group) and m32* ($C2$ space group) and two tetragonal t32 (P-42_1C space group) and t32* ($P4_32_12$ space group)—through the *ab initio* random structure searching (AIRSS) approach using the CASTEP code [19–21]. To date it has only been possible to synthesize small material quantities in microexplosion experiments. Nanocrystals ∼10–100 nm in size have been observed in a mixture of other Si phases, making detailed characterization of fundamental physical properties of these new structures extremely challenging.

Si under increased pressure undergoes a sequence of phase transitions, some of which have been identified only recently [3,7,8,15,22–24]. A peculiar property of Si is that upon decompression, the transition to the ambient diamond cubic (dc-Si, *Fd-3m* space group) state is not fully reversible: the β-Sn-Si phase transforms under static conditions into r8-Si, a narrow band-gap semiconductor [17] at around 9 GPa. In turn, from about 2 GPa, the r8-Si transforms to bc8-Si, a semimetal [25]. These phases commonly coexist at ambient conditions. However, a form of amorphous Si (*a*-Si) can also result during relatively rapid decreases in pressure in a DAC or during nanoindentation [26,27].

In this paper, Raman microspectroscopy is conducted across arrays of laser-induced microexplosion sites in the search of the Raman signatures of new metastable Si phases. We present Raman spectra from modifications created from 35 to 150 J/cm^2 of laser fluence, and we discuss the observed Raman features. Alongside strong signals from compressed dc-Si and *a*-Si, we observe peaks that correlate with a number of known phases, including r8-Si and bc8-Si, peaks that are suggestive of twinlike stacking, and also peaks that do not match any described Si phases, and potentially including st12-Si and/or bt8-Si.

II. EXPERIMENTAL RESULTS

Ultrafast laser-induced microexplosion experiments were performed using 170-fs, 790-nm, 1-kHz repetition rate laser pulses from a Ti-sapphire MXR-2001 CLARK laser system. The laser pulses with energy up to 2.5 μJ were tightly focused onto a silicon surface protected by a 10-μm-thick transparent oxide layer. Each of the regions was irradiated by a single laser pulse with energy in the range from 150 to 700 nJ, which corresponds to a fluence range from 35 to 150 J/cm^2 on the Si surface. Below this energy range, the microexplosion conditions were not sufficient to produce a strong shock wave with a pressure above Young's modulus of SiO$_2$ and Si (∼75 and ∼165 GPa, respectively) and thus to form a void surrounded by compressed material. The laser-modified sites of approximately 0.3–0.75 μm in size can be clearly optically detected; see Fig. 1(a). The appearance of cracks between the sites has been observed with increasing fluence, becoming common above 150 J/cm^2. Thus, this fluence level determined the practical upper limit for the deposited laser energy in our experiments. The details of the experimental setup are described in Ref. [3] and the Supplemental Material [28].

A. Observation of amorphous silicon

The high-intensity ultrashort laser pulses deliver energy density up to several MJ/cm^3 and induce a dense nonequilibrium plasma state in which crystallinity is completely lost. The submicron size of the modified sites subsequently allows rapid quenching via electronic heat conduction and the overcoming of kinetic barriers to the formation of metastable polymorphs, which are preserved in a surrounding compressed shell [3,4].

At low fluence the quenching time is shorter than the time required for a crystal to grow, resulting in *a*-Si [3]. Typical results of Raman mapping of microexplosion sites made at 35 J/cm^2 are presented in Figs. 1(b) and 1(c). The maps were produced of the same sites using the Raman spectral ranges associated with dc-Si in Fig. 1(b) and *a*-Si in Fig. 1(c), while the corresponding Raman spectra are in Fig. 1(d). Mapping the same area using different Raman frequencies, one correlated with *a*-Si and another one with dc-Si, demonstrates clearly that *a*-Si dominates within the laser-modified sites, which are surrounded by a pristine dc-Si matrix.

As fluence increases, so does the modification size; see Figs. 1(e) and 1(f). Each modification is visible with a dark dot at the center, with a ring of *a*-Si around it. Crystal growth within the modified region becomes increasingly favored under higher laser fluence. At 95 J/cm^2 [Fig. 2(e)], the void at the center of the modification is large enough to be resolved, resulting in an apparent ring of *a*-Si. Finally, at 130 J/cm^2 [Fig. 2(f)], the modifications are so large that the laser processed sites start to merge and *a*-Si tends to disappear. The SiO$_2$ had no observable influence on the Raman spectra collected, nor is there evidence of high-density oxides.

B. Raman signatures of metastable silicon phases

A typical Raman spectrum, recorded from laser-induced microexplosion sites at a laser fluence of 95 J/cm^2, is presented in Fig. 2, and that at 65 J/cm^2 is presented in Fig. 3. The labeled peak positions are given in Table I.

III. DISCUSSION

A. Estimation of residual stress

Given that modifications are created by a microexplosion with a compressive shockwave, it is no surprise that evidence of compression is observable by Raman spectroscopy. Several peaks beyond those of *a*-Si and dc-Si are evident in Fig. 2(a), namely at 522 and 539 cm^{-1}, and they can be explained by compressive strain, which is known to cause the TO band of dc-Si to shift to higher wave numbers [29–32]. Furthermore, this shift in peak position can be related to compressive strain using Eq. (1) [29]:

$$\Delta\omega_{\text{dc-Si}}^{\text{TO}} = 518.6 + 0.55P - 8.66 \times 10^{-4}P^2, \qquad (1)$$

where $\Delta\omega_{\text{dc-Si}}^{\text{TO}}$ is the Raman shift (in cm^{-1}) and P is the pressure (in kbar). Inhomogeneity of strain throughout the sampled volume required three separate curves to more
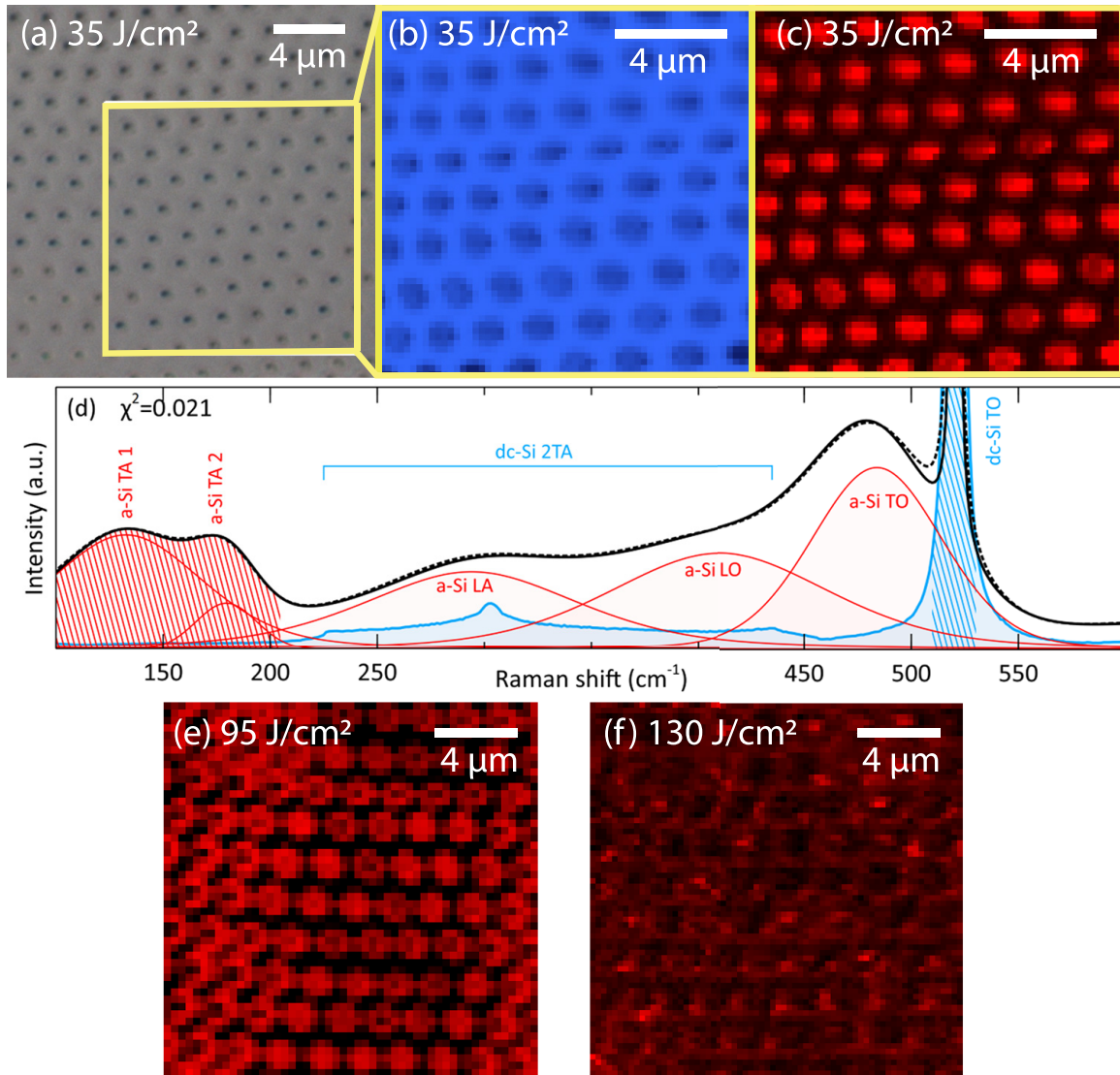
FIG. 1. Optical image (a) and Raman (b), (c), (e), (f) mapping of modifications induced on the Si-surface with different laser fluences from 35 to 130 J/cm^2. (b) Raman map of the sites formed at 35 J/cm^2 taken in the 510–530 cm^{-1} range and showing the dc-Si distribution. The map is coded in blue in correlation with the frequency range shown in (d). (c) a-Si mapping of the same area taken in the 100–205 cm^{-1} range, colored in red and marked in (d); Raman images of the a-Si distribution of the sites produced at 95 J/cm^2 (e) and 130 J/cm^2 (f).

accurately fit the TO band. These are centered at unstrained 520 cm^{-1} and strained 522 and 539 cm^{-1} values that correspond in the latter cases to $\sim$0.7 and $\sim$4 GPa compressive stress, respectively. Furthermore, both strained peaks are significantly broadened relative to the unstrained peak, further indicating inhomogeneity. Using Eq. (1), residual compressive stresses of over 4.5 GPa have been estimated from the dc-Si TO peak in this study.

The ability to maintain a remnant compressive stress in the dc-Si of the order of 4 GPa is, however, significant. Assuming similar remnant stress within the other Si phases, this raises the prospect of the existence of highly compressed a-Si (that is, high-density a-Si [33,34]) and the possibility of preserved r8-Si without the coexistence of bc8-Si. Although a residual pressure of $\sim$4 GPa may seem high, this pressure is similar to that reported in recent work in which phase transformations in Si were induced via single axis loading using nanoindentation and a diamond tip [35]. This study revealed that the residual

stresses allow the r8-Si phase to be dominant in the recovered material. It is thus conceivable that some of the novel phases created in the far-from-equilibrium conditions of this work also require large remnant stresses to be preserved in the sample after laser modification. Large residual stress will clearly impact the properties (electrical and optical) of novel phases.

B. Laser-induced crystalline phases

The crystalline phase assignments of the Raman P1-P6 peaks, observed in Fig. 2(a) for 95 J/cm^2, are shown in Table I alongside bc8-Si and r8-Si peak positions from the literature. Note that as these phases often coexist and have many similar Raman features, phonon mode assignment can be difficult. The 3 GPa values are obtained from [36], where the ambient pressure values have been normalized to the indentation data [37] and the 3 GPa peak positions shifted accordingly.

FIG. 2. (a) Experimental Raman spectrum collected under confocal conditions from modifications created at 95 J/cm^2 laser fluence, which contains *a*-Si (in red) and dc-Si (in blue), and peaks from compressed dc-Si and crystalline metastable phases (labeled as P1–P6). The peak positions are given in Table I. (b)–(d) Computed Raman spectra for r8-Si (b), bc8-Si (c), and bt8-Si (d).
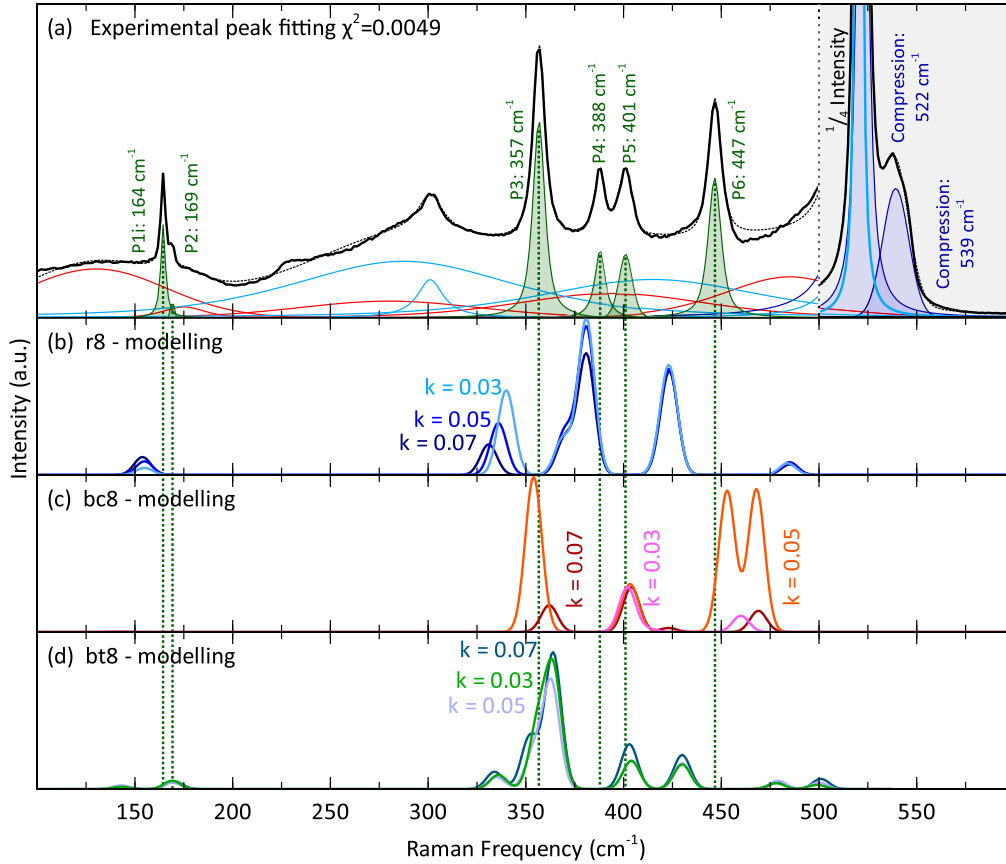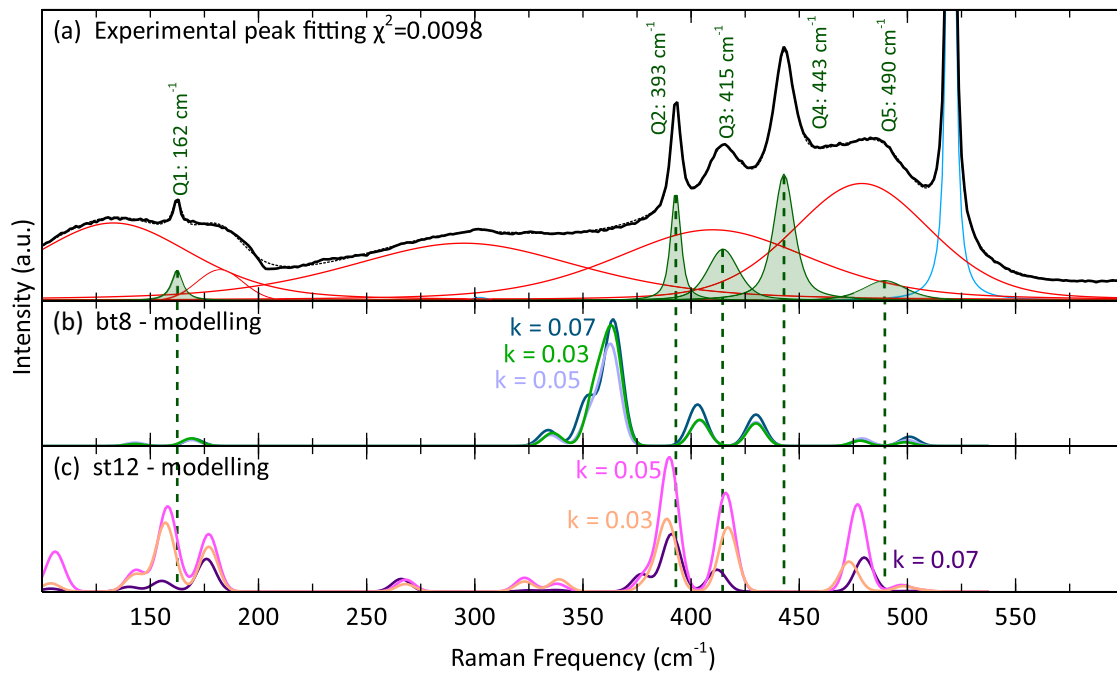

FIG. 3. (a) Raman spectrum collected under confocal conditions from modifications created at 65 J/cm^2 laser fluence, which contains *a*-Si (red) and dc-Si (blue), and peaks from additional crystalline metastable phases (labeled as Q1–Q5). The peak positions are given in Table I. (b), (c) Computed Raman spectrum corresponding to bt8-Si (b) and st12-Si (c).

TABLE I. Peak positions from 65 and 95 J/cm² experiments as well as a selection of the closest matching bc8-Si (Si-III) and r8-Si (Si-XII) peaks from high-pressure DAC measurements at 3 GPa [36] and 3.5 GPa [38]. The 3 GPa results are normalized to unloaded indentation data [37].

Laser-induced microexplosion at 65 J/cm²		Laser-induced microexplosion at 95 J/cm²		Values from the literature Peak position (cm⁻¹)			Phase/ symmetry
Peaks (cm⁻¹)		Peaks (cm⁻¹)		DAC 3 GPa [36]	DAC 3.5 GPa [38]	After indentation [37]	[37]
Q1	162	P1	164	163	164	165	r8/A_g
		P2	169	168		170	r8/E_g
		P3	357	357	358	352	r8/A_g
Q2	393	P4	388	388	387	384	bc8/T_g
		P5	401	402	401	397	r8
Q3	415			426		412	bc8
Q4	443	P6	447	448	447	438	bc8/E_u
Q5	490			518	503	∼470 (broad) a-Si	r8 [35]

The 3.5 GPa values are direct measurements from [38]. The experimentally obtained peaks correlate well to those created by DAC with a 3-3.5 GPa external pressure after unloading to ambient pressure, and they are in agreement with the predominantly r8-Si recovered from indentation loading [35]. It is noteworthy that at such elevated pressures, additional phonon modes, absent in this work, are generally evident in DAC studies, such as in the low-wave-number region. Thus, the similarity of the observed peak positions to those of r8-Si and bc8-Si at moderate pressure suggests that a mixture of r8-Si and bc8-Si phases is present at residual pressures between 3.0 and 3.5 GPa. Reference [24] proposes that the structurally similar phases of r8, bc8, and bt8 are highly likely to coexist. Hence, the Raman spectrum in Fig. 2 may well contain all of these phases.

C. Novel Si signatures

The Raman spectrum, recorded from laser-induced microexplosion modifications created at a laser fluence of 65 J/cm², is presented in Fig. 3, and the labeled peak positions are given in Table I. It contains the peaks listed as Q1–Q5 [Fig. 3(a) and Table I] that resemble r8 and bc8 Raman peaks from the literature, but the prevalent r8-Si peak located at ∼357 cm⁻¹ is absent in the spectrum. This is suggestive of highly deformed bc8-Si or similarly the presence of bt8-Si. In our previous TEM study [3], we observed the st12-Si phase in sites created at a laser fluence of 48 J/cm², bt8-Si at 95 J/cm², and the study also revealed several diffraction spots that could not be indexed to known Si phases. DFT modeling has suggested some possibilities, namely the monoclinic m32 and m32* structures and the tetragonal t32 and t32* structures [3]. Nevertheless, correlated TEM and Raman analysis, coupled with DFT modeling, may be needed to help identify any possible novel metastable allotropes of Si.

The metastable phases of Si are such narrow-band-gap materials, and this presents a challenge to the computation of the Raman spectra. The density functional theory (DFT) is well known to underestimate electronic band gaps, and, for the case of narrow-gap systems, it can even predict a metallic state. In an attempt to mitigate this aspect, we did not allow partial occupancy of the electronic energy levels, and we present our results for a range of Brillouin zone sampling densities: $k = 0.03 \times 2\pi/\text{Å}$, $0.05 \times 2\pi/\text{Å}$, and $0.07 \times 2\pi/\text{Å}$. Comparing the computed spectra for these different sampling densities allows us to assess the impact of metallization due to the limitations of DFT.

The spectra predicted using the CASTEP code [21,28,39–41] are presented as broadened by a Gaussian with a width of $10 \, \text{cm}^{-1}$ for r8-Si, bc8-Si, and bt8-Si in Figs. 2(b)–2(d), and for bt8-Si and st12-Si in Figs. 3(b) and 3(c). The peak positions are well described in all cases, but the Raman intensities are sensitive to the quality of the sampling, in particular for the bc8 and st12 structures, and the peak around $330 \, \text{cm}^{-1}$ for the r8 structure. Although the peak positions in the simulated spectra are in a similar wave-number range to those in the experimental spectra, the match is not perfect for a number of reasons. First, DFT gives only approximate peak positions, and around a 10% shift in the absolute peak positions is to be expected, particularly for narrow-band-gap phases. Second, the spectra have been computed for structures relaxed at 0 GPa, but we demonstrated that the phases observed are under possible residual pressure. This would lead to further shifts in the peak positions and changes in the Raman intensities for computed spectra. Finally, there may be further phases of Si, for example the t32 and m32 phases described in Ref. [3], which should also be considered as having possible contributions to the experimental Raman spectra in Figs. 2(a) and 3(a). As a result, it is difficult to unequivocally assign the observed peaks to any of the phases calculated here. Nevertheless, the calculated peaks for r8, bc8, and bt8 occur in the same wave-number range as the experimental values (particularly in the 350–460 cm⁻¹ range). Based on the similarity of calculated r8, bc8, and bt8 Raman signatures, it is not possible to determine if bt8-Si is present or not, and indeed to distinguish between these three structurally similar tetragonal phases in Raman spectra. In summary, since bt8-Si was observed in TEM cross sections in our previous study [3], we suggest that the Raman spectrum [Fig. 2(a)] may contain this phase, as well as r8-Si and bc8-Si, although it is impossible to determine the phase fractions of each of these phases.

FIG. 4. Raman spectra collected under confocal conditions from a modification created at 95 J/cm^2 laser fluence. (a) The entire spectrum is shown as recorded (in gray), and with the *a*-Si component removed (in black). (b) The region of interest with *a*-Si subtracted (solid black line), and the individual curves for the additional fitted peaks (in purple).

In Fig. 3 the Q peaks are compared to the modeling of bt8-Si and st12-Si. The bt8 modeling (b) resembles the Q peaks assuming that the bt8 peaks shift in a similar manner to the r8/bc8 due to residual stress. Thus, it is plausible that the experimental spectrum contains strained bt8-Si. It is worth examining the calculated st12-Si peak positions in Fig. 3(c) and Table I. The peaks located at 162 cm^{-1} (Q1), 393 cm^{-1} (Q2), and 415 cm^{-1} (Q3) correlate reasonably well, but those at 433 cm^{-1} (Q4) and 490 cm^{-1} (Q5) do not. Further insight here can be gained by scaling the mass of known st12-Ge Raman peaks to estimate those of st12-Si based on the method of Bermejo and Cardona [42]. Indeed, using Eq. (1) in Ref. [43], and the experimental st12-Ge Raman data from Huston *et al.* [44], the estimated st12-Si spectrum was found to be in general agreement with the calculated st12-Si peak positions, but it does not fit the calculated spectrum or rescaled germanium st12 in detail. If the experimental spectrum does contain the st12-Si structure, this inconsistency is again most likely due to residual stress. However, it is also highly likely that the experimental Raman spectrum in Fig. 3 contains an as yet unidentified Si polymorph.

D. Evidence of **9R** polytype

In addition to the crystalline phases described above, there were also many instances in which two peaks located at 495 and 517 cm^{-1} were observed, as shown in Fig. 4, in microexplosion sites created at a fluence of 95 J/cm^2. These peaks overlap with both the *a*-Si TO band and the dc-Si TO band, and they proved difficult to fit accurately. To aid the interpretation, a suitably scaled strongly *a*-Si spectrum, similar to Fig. 1(d), is subtracted away from the recorded spectrum. The resultant curve fit for the region of interest is presented in Fig. 4(b). These peaks could be associated with hexagonal diamond Si (hd-Si $P6_3/mmc$ space group), which has been widely reported to form after annealing of a mixture of r8 and bc8 and exhibits similarly located Raman peaks [45]. However, the 9R polytype (stacking ABCBCACAB …) has been shown to have a similar Raman signature [46], and the TEM selected area diffraction from this region, shown in Fig. 5, shows a characteristic pattern of the 9R polytype, the [01$\bar{1}$] zone axis diffraction pattern of Si with the additional diffraction spots at 1/3 increments of the {111} spots.

FIG. 5. (a) TEM micrograph of a modification created by a laser microexplosion at 150 J/cm^2; (b) a higher magnification of the Si region showing a characteristic 9R stacking pattern; and (c) the corresponding TEM selected area diffraction pattern, with (d) its indexing of the [01$\bar{1}$] zone axis. Filled circles indicate forbidden reflections due to double reflections; crosses indicate the satellites by stacking.

Of these two possibilities (hd-Si and $9R$ stacking), the former is considered unlikely for the following reasons. hd-Si is known to arise from the thermal annealing of bc8-Si at temperatures around $200\,°C$. After laser irradiation, the fast temperature quenching of the submicron-sized modified zone indicates that the Si will essentially cool down to the solidification temperature in ~ 27 ns after the laser irradiation. Taking into account the speed of crystallization as 15.5 m/s [47], the $1\,\mu m$ Si modification is crystallized in ~ 65 ns, and it returns to ambient temperature in about 5 μs (see the Supplemental Material of [3]). Thus, hd-Si is unlikely to arise from thermal annealing of bc8 during or following the laser-induced microexplosion. In terms of heating during Raman analysis, this only had an observable influence with both greatly prolonged exposure times, and an order of magnitude higher laser power than was used for the results presented here. Finally, as stated and shown in Fig. 5, $9R$ stacking was observed by TEM in samples exhibiting Raman peaks at 495 and $517\,cm^{-1}$, making a result of $9R$ stacking much more plausible.

The question is how $9R$ stacking might arise in dc-Si in this study, and we suggest that it might be stress-induced and occur in dc-Si surrounding the highly compressed laser-modified zone. Indeed, pulsed laser melting of Si in the ns regime has shown TEM diffraction patterns with the 1/3 spacing suggestive of $9R$ stacking [48].

IV. CONCLUSIONS

This work has demonstrated that precise and controlled microexplosions created in a confined volume of Si by femtosecond laser irradiation lead to a variety of high-pressure Si allotropes. The main phase component observed in most modifications is a-Si, arising from rapid quenching at shorter cooling times, and this phase dominates at low laser fluences. As laser fluence increases, the modified material surrounding the void increases in volume and contains an increasing fraction of compressed crystalline Si phases. Such compression can lead to significant residual stress in the modifications, measured at up to 4.5 GPa from the Raman shift of the main dc-Si peak. Since the a-Si component is normally found adjacent to this compressed crystalline region, it almost certainly exhibits a higher density than relaxed a-Si under ambient conditions.

Raman microspectroscopy has revealed several crystalline Si allotropes in addition to compressed dc-Si. We have demonstrated the presence for the structurally similar phases r8-Si, bc8-Si, and plausibly bt8-Si or st12-Si, but it is im-

possible to determine the phase fractions of these phases from the Raman data. The r8 and bc8-Si crystalline allotropes have previously been observed in near-equilibrium DAC and indentation experiments, while bt8 and st12 were observed in microexplosion modifications using TEM, as were several additional phases such as m32, m32*, t32, and t32*. All these phases have interesting electrical properties of relevance for electronic applications. The absence of a clear correlation with the unknown component in Fig. 3 is evidence of an as yet unidentified Si phase. Recently published theoretical calculations [23] indicate a family of very similar structures that could contribute to the spectra we observed in our experiments. In addition, we have demonstrated the presence of the $9R$ polytype in dc-Si, revealed by the Raman signatures of $9R$ stacking and TEM analysis.

This study shows that residual stress is essential in stabilizing metastable Si allotropes, which could be critical in prospective applications. Clearly, in order to identify such phases, there is a need for correlated TEM, Raman, and XRD studies of modifications, along with DFT modeling.

[1] S. Juodkazis, K. Nishimura, S. Tanaka, H. Misawa, E. G. Gamaly, B. Luther-Davies, L. Hallo, P. Nicolai, and V. T. Tikhonchuk, Phys. Rev. Lett. **96**, 166101 (2006).

[2] E. G. Gamaly, S. Juodkazis, K. Nishimura, H. Misawa, B. Luther-Davies, L. Hallo, P. Nicolai, and V. T. Tikhonchuk, Phys. Rev. B **73**, 214101 (2006).

[3] L. Rapp, B. Haberl, C. J. Pickard, J. E. Bradby, E. G. Gamaly, J. S. Williams, and A. V. Rode, Nat. Commun. **6**, 7555 (2015).

[4] A. Vailionis, E. G. Gamaly, V. Mizeikis, W. Yang, A. V. Rode, and S. Juodkazis, Nat. Commun. **2**, 445 (2011).

[5] E. G. Gamaly, A. Vailionis, V. Mizeikis, W. Yang, A. V. Rode, and S. Juodkazis, High Energy Density Phys. **8**, 13 (2012).

[6] E. G. Gamaly, L. Rapp, V. Roppo, S. Juodkazis, and A. V Rode, New J. Phys. **15**, 025018 (2013).

[7] Q. Zhu, A. R. Oganov, A. O. Lyakhov, and X. Yu, Phys. Rev. B **92**, 024106 (2015).

[8] M. Amsler, S. Botti, M. A. L. Marques, T. J. Lenosky, and S. Goedecker, Phys. Rev. B **92**, 014101 (2015).

[9] A. Y. Vorobyev and C. Guo, Opt. Express **19**, A1031 (2011).

[10] B. Haberl, T. A. Strobel, and J. E. Bradby, Appl. Phys. Rev. **3**, 040808 (2016).

[11] M. J. Smith, M.-J. Sher, B. Franta, Y.-T. Lin, E. Mazur, and S. Gradečak, J. Appl. Phys. **112**, 083518 (2012).

[12] C. H. Crouch, J. E. Carey, M. Shen, E. Mazur, and F. Y. Génin, Appl. Phys. A **79**, 1635 (2004).

[13] E. Ertekin, M. T. Winkler, D. Recht, A. J. Said, M. J. Aziz, T. Buonassisi, and J. C. Grossman, Phys. Rev. Lett. **108**, 026401 (2012).

[14] L. Rapp, B. Haberl, J. E. Bradby, E. G. Gamaly, J. S. Williams, and A. V. Rode, Appl. Phys. A **114**, 33 (2014).

[15] J.-T. Wang, C. Chen, H. Mizuseki, and Y. Kawazoe, Phys. Rev. Lett. **110**, 165503 (2013).

[16] V. E. Dmitrienko, M. Kleman, and F. Mauri, Phys. Rev. B **60**, 9383 (1999).

[17] B. D. Malone, J. D. Sau, and M. L. Cohen, Phys. Rev. B **78**, 035210 (2008).

[18] J. D. Joannopoulos and M. L. Cohen, Phys. Rev. B **7**, 2644 (1973).

[19] C. J. Pickard and R. J. Needs, Phys. Rev. Lett. **97**, 045504 (2006).

[20] C. J. Pickard and R. J. Needs, J. Phys. Condens. Matter **23**, 053201 (2011).

[21] S. J. Clark, M. D. Segall, C. J. Pickard, P. J. Hasnip, M. I. J. Probert, K. Refson, and M. C. Payne, Z. Krist. Mater. **220**, 567 (2005).

[22] A. Mujica, A. Rubio, A. Munõz, and R. J. Needs, Rev. Mod. Phys. **75**, 863 (2003).

[23] A. Mujica, C. J. Pickard, and R. J. Needs, Phys. Rev. B **91**, 214104 (2015).

[24] V. E. Dmitrienko and V. A. Chizhikov, Phys. Rev. B **101**, 245203 (2020).

[25] H. Zhang, H. Liu, K. Wei, O. O. Kurakevych, Y. Le Godec, Z. Liu, J. Martin, M. Guerrette, G. S. Nolas, and T. A. Strobel, Phys. Rev. Lett. **118**, 146601 (2017).

[26] N. Garg, K. K. Pandey, K. V. Shanavas, C. A. Betty, and S. M. Sharma, Phys. Rev. B **83**, 115202 (2011).

[27] V. Domnich, Y. G. Gogotsi, and S. Dub, Appl. Phys. Lett. **76**, 2214 (2000).

[28] See Supplemental Material at http://link.aps.org/supplemental/10.1103/PhysRevMaterials.4.093803 for a detailed description of the experimental conditions, Raman micro-spectroscopy, DFT calculations of Si phases, and TEM images and diffraction pattern recording.

[29] T. P. Mernagh and L.-G. Liu, J. Phys. Chem. Solids **52**, 507 (1991).

[30] V. Paillard, P. Puech, M. A. Laguna, P. Temple-Boyer, B. Caussat, J. P. Couderc, and B. de Mauduit, Appl. Phys. Lett. **73**, 1718 (1998).

[31] H. Richter, Z. P. Wang, and L. Ley, Solid State Commun. **39**, 625 (1981).

[32] V. Paillard, P. Puech, M. A. Laguna, R. Carles, B. Kohn, and F. Huisken, J. Appl. Phys. **86**, 1921 (1999).

[33] F. Wooten, K. Winer, and D. Weaire, Phys. Rev. Lett. **54**, 1392 (1985).

[34] E. Holmström, B. Haberl, O. H. Pakarinen, K. Nordlund, F. Djurabekova, R. Arenal, J. S. Williams, J. E. Bradby, T. C. Petersen, and A. C. Y. Liu, J. Non-Cryst. Solids **438**, 26 (2016).

[35] S. Wong, B. Haberl, B. C. Johnson, A. Mujica, M. Guthrie, J. C. McCallum, J. S. Williams, and J. E. Bradby, Phys. Rev. Lett. **122**, 105701 (2019).

[36] H. Olijnyk and A. P. Jephcoat, Phys. Status Solidi **211**, 413 (1999).

[37] B. C. Johnson, B. Haberl, J. E. Bradby, J. C. McCallum, and J. S. Williams, Phys. Rev. B **83**, 235205 (2011).

[38] M. Hanfland and K. Syassen, High Press. Res. **3**, 242 (1990).

[39] K. Refson, P. R. Tulip, and S. J. Clark, Phys. Rev. B **73**, 155114 (2006).

[40] J. P. Perdew, A. Ruzsinszky, G. I. Csonka, O. A. Vydrov, G. E. Scuseria, L. A. Constantin, X. Zhou, and K. Burke, Phys. Rev. Lett. **100**, 136406 (2008).

[41] G. P. Francis and M. C. Payne, J. Phys. Condens. Matter **2**, 4395 (1990).

[42] D. Bermejo and M. Cardona, J. Non. Cryst. Solids **32**, 405 (1979).

[43] B. C. Johnson, B. Haberl, S. Deshmukh, B. D. Malone, M. L. Cohen, J. C. McCallum, J. S. Williams, and J. E. Bradby, Phys. Rev. Lett. **110**, 085502 (2013).

[44] L. Q. Huston, B. C. Johnson, B. Haberl, S. Wong, J. S. Williams, and J. E. Bradby, J. Appl. Phys. **122**, 175108 (2017).

[45] H. I. T. Hauge, M. A. Verheijen, S. Conesa-Boj, T. Etzelstorfer, M. Watzinger, D. Kriegner, I. Zardo, C. Fasolato, F. Capitani, P. Postorino, S. Kölling, A. Li, S. Assali, J. Stangl, and E. P. A. M. Bakkers, Nano Lett. **15**, 5855 (2015).

[46] F. J. Lopez, E. R. Hemesath, and L. J. Lauhon, Nano Lett. **9**, 2774 (2009).

[47] H.-D. Geiler, E. Glaser, G. Götz, and M. Wagner, J. Appl. Phys. **59**, 3091 (1986).

[48] W. Yang, A. J. Akey, L. A. Smillie, J. P. Mailoa, B. C. Johnson, J. C. McCallum, D. Macdonald, T. Buonassisi, M. J. Aziz, and J. S. Williams, Phys. Rev. Mater. **1**, 74602 (2017).

[49] http://energy.gov/downloads/doe-public-access-plan